

Inhibition of copper corrosion in aerated hydrochloric acid solution by amino-acid compounds

DA-QUAN ZHANG*, LI-XIN GAO and GUO-DING ZHOU

Electrochemical Research Group, Shanghai University of Electric Power, Shanghai, 200090, P. R. China

(*author for correspondence, fax: +86-21-6570-0719; e-mail: zhdq@public9.sta.net.cn)

Received 6 September 2004; accepted in revised form 7 June 2005

Key words: amino-acid compounds, copper, corrosion inhibition, HCl solution

Abstract

The effect of two amino-acid compounds, DL-alanine and DL-cysteine, on copper corrosion in an aerated 0.5 mol l⁻¹ HCl solution was studied by weight-loss measurements, potentiodynamic polarisation curves, and electrochemical impedance spectroscopy. A conventional benzotriazole (BTA) inhibitor was also tested for comparison. DL-cysteine was shown to be the most effective inhibitor among those tested inhibitors. Potentiodynamic polarisation results revealed that both the DL-alanine and DL-cysteine acted as an anodic inhibitor; however, DL-cysteine, in particular, was more effective, as it strongly suppressed anodic current densities. The improved inhibition efficiency of DL-cysteine in the 0.5 mol l⁻¹ HCl solution was due to its adsorption on the copper surface via the mercapto group in its molecular structure.

1. Introduction

Copper is a relatively noble metal, but can suffer severe corrosion in aerated acidic media. One of the most important methods in the corrosion protection of copper is the use of organic inhibitors. Nitrogen-containing and sulphur-containing organic heterocyclic compounds may act as inhibitors for copper dissolution due to the chelating action of heterocyclic molecules and the formation of a physical blocking barrier on the copper surface [1, 2]. Among organic heterocyclic compounds, benzotriazole (BTA) is well known as an effective inhibitor of copper corrosion in neutral/alkaline solutions [3, 4]. It is generally accepted that its inhibition mechanism in neutral and alkaline solution is the adsorption of single BTA molecules on the copper surface and the formation of a polymeric film of a (Cu⁺BTA) complex [5]. However, in an acidic solution, BTA exists predominantly as a protonated species, BTAH⁺. This protonated species is less strongly chemisorbed on the copper surface, as the metal is thought to be positively charged in acidic solution [6]. This in turn leads to a decrease in the inhibition efficiency of BTA in acidic solution. There is a need for new inhibitors for copper corrosion in acidic media.

A possible solution to this problem is to synthesize a BTA derivative having greater inhibitory activity than that of the parent BTA molecule. Schweinsberg et al. have done extensive research on the action of benzo-

triazole and its derivatives for copper corrosion in acidic solutions [7–9]. Some other heterocyclic compounds have also been shown to be effective inhibitors of the corrosion of copper and its alloys. These include 2-mercaptobenzothiazole (MBT) [10, 11], and bis-(1-benzotriazolymethylene)-(2,5-thiadiazoly)-disulfide [12]. However, a very important disadvantage of these heterocyclic compounds is their toxicity and most of them cannot be biodegraded [13]. This lack of biodegradability leads to the emission of industrial waste water carrying a large amount of toxic material to public waterways. Toxic inhibitors that are used widely in industrial processes must be replaced with new ecologically friendly inhibitors [14].

Amino-acid derivatives are of particular importance as corrosion inhibitors, because they are environmentally friendly and have very low toxicity. Moretti et al. reported tryptamine as a green iron corrosion inhibitor in 0.5 mol l⁻¹ deaerated sulphuric acid [15]. In the present study, the efficiency of two kinds of amino-acid compounds for the inhibition of copper corrosion in a 0.5 mol l⁻¹ HCl solution was investigated. The amino-acid compounds are DL-alanine and DL-cysteine, and their structures are shown in Figure 1.

The inhibition efficiencies were determined by coupon tests. Corrosion inhibition was investigated by means of potentiodynamic polarisation curves and electrochemical impedance spectroscopy (EIS). The results are compared with those obtained using the conventional BTA inhibitor.

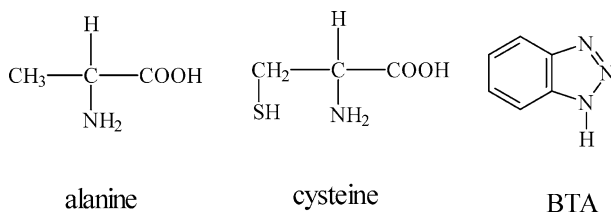


Fig. 1. Molecular structure of corrosion inhibitors.

2. Experimental

2.1. Materials and chemicals

The specimens used for weight-loss measurements were circular copper discs ($\phi 4.0 \times 0.15$ cm), and the calculated exposed specimen surface area was 25.04 cm^2 . The working electrode (WE) for the potentiodynamic polarisation curves and EIS measurements was prepared from a cylindrical copper rod (99.99%) sealed with epoxy resin, while the circular cross section (0.4 cm^2) of the rod was exposed. Amino-acid compounds and BTA were AR grade and used as received, while all other chemicals were AR grade. Finally, solutions were prepared using deionized water.

2.2. Apparatus

Weight-loss measurements were conducted by suspending the coupons in a 1000 ml vessel with 400 ml of test solution, and the vessel was placed in a thermostat water bath. Electrochemical measurements were performed in a three-electrode cell using a PARC M283 potentiostat (EG&G) with a PC. A PARC Model 1025 frequency response analyzer was also used for the EIS measurements. M352 and M398 software packages were used to obtain the polarisation curves and electrochemical impedance spectra, respectively.

2.3. Procedures

2.3.1. Weight-loss measurements

The coupons were abraded with emery paper of different grades (#1, #4, and #6), washed and degreased with alcohol, and dried and rinsed with deionized water. The coupons with freshly prepared surfaces were then fully immersed in quiescent 0.5 mol l^{-1} HCl test solutions for 4 days at 40°C . All solutions were exposed to air, and after the corrosion test, the corrosion products were removed from the metal surface by the hard rubber. The coupons were then rinsed in deionized water and dried. The mean corrosion rates (CRs) and inhibition efficiencies (IEs) over the exposure period were calculated using the following equations:

$$\text{CR} = \frac{W_0 - W_1}{A \times T} \quad (1)$$

$$\text{IE\%} = \frac{\text{CR}_1 - \text{CR}_2}{\text{CR}_1} \times 100\% \quad (2)$$

where CR is in $\text{g m}^{-2} \text{ h}^{-1}$; A is the specimen area (m^2); W_0 is the original weight (g) of the specimen; W_1 is the specimen weight (g) after the immersion period; T is the immersion period (h); and CR_1 and CR_2 are the corrosion rates without and with an inhibitor, respectively.

2.3.2. Potentiodynamic polarisation measurements

A three-electrode cell, employing a copper rod-working electrode (WE), platinum foil counter electrode, and saturated calomel electrode reference electrode (SCE) was used for measurements. The WE was abraded with 1200 and 2000 emery paper, which was degreased with AR-grade ethanol and acetone, and then rinsed with deionized water prior to each experiment. The degreased WE was inserted into the solution. After 30 min of immersion, the potential was stable E_{corr} . The electrode was then polarised from -800 mV to $+700 \text{ mV}$ at 1 mV s^{-1} . The cell was open to the laboratory air, and measurements were conducted at room temperature. All potentials are presented in mV (SCE).

2.3.3. Electrochemical impedance measurements

The EIS experiments were performed at open circuit potential over a frequency range of 0.05 Hz to 100 kHz. The sinusoidal potential perturbation was 5 mV in amplitude. During the measurements, the solution was not stirred or deaerated.

3. Results and discussion

3.1. Weight-loss measurements

The average corrosion rates and the percentages of inhibition efficiencies (IE%) are shown in Table 1. All the compounds used inhibited the corrosion of copper in the 0.5 mol l^{-1} HCl solution. Both alanine and cysteine showed better protection than BTA. Cysteine, which contains a mercapto group in its molecular structure, was the most effective among the inhibitors tested, while alanine was less effective than BTA.

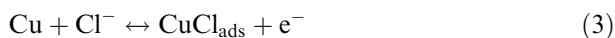
3.2. Polarisation curve measurements

Figure 2 shows typical polarisation curves for copper in aerated 0.5 mol l^{-1} HCl solution with and without an inhibitor.

Table 1. Calculated corrosion rates ($\text{g m}^{-2} \text{ h}^{-1}$) and inhibition efficiencies (%) in weight-loss tests

Inhibitors	Mass loss/g	Corrosion rate/ $\text{g m}^{-2} \text{ h}^{-1}$	Inhibition efficiency/%
Blank	1.1351	4.722	–
$10^{-5} \text{ mol l}^{-1}$ Alanine	0.6507	2.707	42.7
$10^{-5} \text{ mol l}^{-1}$ Cysteine	0.4689	1.951	58.7
$10^{-5} \text{ mol l}^{-1}$ BTA	0.7237	3.011	36.2

Anodic dissolution of copper in chloride media has been studied extensively [16, 17]. The mechanisms of anodic dissolution of copper in acidic chloride solutions are:



The anodic curve for the copper electrode in a 0.5 mol l⁻¹ HCl blank solution exhibits two limiting current plateaus. This indicates the role of a diffusion-limiting step, probably both the transport of chloride (Cl⁻) to the surface and the diffusion of (CuCl₂) in the solution. An anodic current peak A appeared at a potential of about -25 mV (SCE) and was related to the CuCl film formation. E_{corr} was -537 mV, -455 mV, and -332 mV for BTA, alanine, and cysteine, respectively. The shapes of the curves in Figure 2 show that the three inhibitors all have inhibitory effects, and the introduction of a mecapto group to the amino-acid compound enhances the inhibitory effect. The three distinct regions that appeared for copper in the presence of cysteine were active dissolution, transition, and limiting current regions. The active region showed apparent Tafel behavior with a slope close to 60 mV [18, 19]. A large decrease in the anodic current density in comparison to the inhibitor-free solution was observed, which indicated that cysteine interacted with the copper surface and inhibited the formation of cuprous complexes [20].

The cathodic corrosion reaction in an aerated acidic chloride solution is



It is clear that the cathodic reaction shows a pseudo-Tafel region with and without organic inhibitor in a 0.5 mol l⁻¹ HCl solution. The cathodic portion of the polarisation curve is a composite and represents copper ion and oxygen reduction. The constancy of this cathodic slope indicates that the mechanism of the cathodic reaction is not changed by the addition of the inhibitor. The total

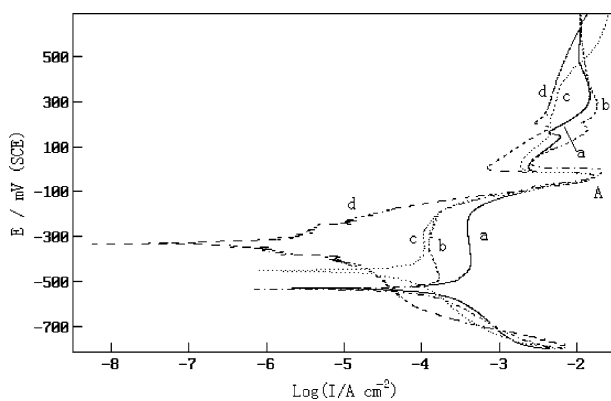
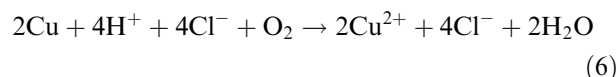


Fig. 2. Polarisation behavior of a copper electrode in 0.5 mol l⁻¹ HCl without (a) and with 10⁻⁵ mol l⁻¹ of BTA (b), alanine (c) or cysteine (d).

corrosion reaction of copper in acidic chloride solutions is as follows:



In general, both alanine and cysteine acted mainly as anodic inhibitors with a shift of E_{corr} to more positive values. They all showed an inhibitive effect on the anodic dissolution of copper. Cysteine showed the best inhibition effect.

3.3. Electrochemical impedance measurements

Impedance measurements on the copper electrode in a 0.5 mol l⁻¹ HCl solution alone and in the presence of inhibitors were performed at open-circuit potential. The Nyquist plots for the copper electrode in the 0.5 mol l⁻¹ HCl solutions without and with inhibitors are shown in Figures 3 and 4. The equivalent circuit models employed for this system are presented in Figure 5. The first equivalent circuit (Figure 5(a)) was used to simulate the EIS data displaying a Warburg impedance, while the second (Figure 5(b)) was used to fit the EIS data displaying a capacitive semicircle. In Figure 5, W stands for the Warburg impedance, R is a resistor (R_s = solution resistance, and R_t = charge transfer resistance), and C_{dl} represents the double layer capacitance.

Figure 3 shows possible Warburg impedance for copper in uninhibited HCl, indicating a diffusion effect [21]. The corrosion behavior of copper in the uninhibited solutions was influenced by mass transport. It is important as to whether the Warburg impedance at the open circuit potential was caused by the anodic oxidation reactions occurring on the copper surface. For the Cu/HCl system, the cathodic reactions and anodic reaction occurring on the copper surface at the open circuit potential were the reduction of O₂ and dissolution of copper, respectively. Despite the fact that oxygen reduction was influenced by mass transport, the mass transport process produced in the anodic copper dissolution predominated at the open circuit potential.

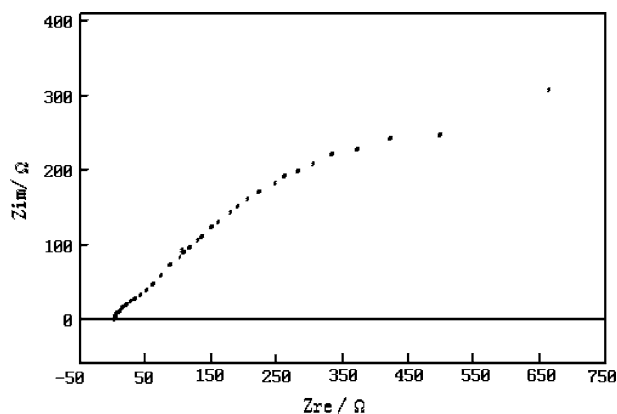


Fig. 3. Nyquist plots of a copper electrode in 0.5 mol l⁻¹ HCl without inhibitors after 4 h immersion.

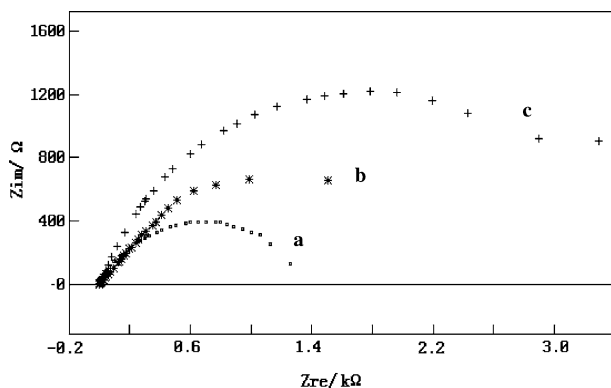


Fig. 4. Nyquist plots of a copper electrode in 0.5 mol l⁻¹ HCl after 4 h immersion containing 10⁻⁵ mol l⁻¹ inhibitors: BTA (a), alanine (b) and cysteine (c).

Recently, the exact definition of the diffusion processes involved in this potential region was discussed and described as being limited by CuCl₂ diffusion [22].

Figure 4 shows the Nyquist impedance diagrams for copper in a 0.5 mol l⁻¹ HCl solution containing BTA, alanine, and cysteine, respectively. A depressed semicircle with its center below the real axis was observed. This phenomenon is known as the dispersing effect [23]. As for cysteine, the corrosion behavior of copper in this solution was influenced, to some extent, by mass transport since the Warburg impedance plot was observed in the low frequency region. Nyquist plots do not show a straight-line portion at low frequencies because of the limited low frequency range. The HF depressed semicircle is proposed to be the time constant of charge transfer and double layer capacitance. Various parameters were obtained by fitting the experimental Nyquist data to a simple semicircle. The HF intercept gives the solution resistance (R_{sol}). The charge transfer resistance (R_t) values were calculated from the difference in impedance at the lower frequency intercept and higher frequency intercept as suggested by Hladky et al. [24]. The double layer capacitance (C_{dl}) was calculated by the following equation:

$$C_{dl} = \frac{1}{wR_t} \quad (7)$$

where w is the angular frequency at which the imaginary component of the impedance is maximum, and R_t represents the charge transfer resistance.

The electrochemical impedance parameters derived from these figures are given in Table 2.

The charge transfer resistance (R_t) in the presence of cysteine was greater than that with alanine or BTA

alone. The smaller the charge transfer resistance, the faster the corrosion rate. The double layer capacitance (C_{dl}) values decreased when the inhibitors were presented in a 0.5 mol l⁻¹ HCl solution. The decrease in the C_{dl} values was due to inhibitor adsorption on the copper surface. These results suggest that cysteine has the best protection effect against copper corrosion among the three compounds. The effect of molecular structure on inhibition efficiency was the same as that determined by using the weight-loss method and electrochemical polarisation measurements. Hence, the results obtained using these three different methods for efficiencies of BTA, alanine and cysteine agreed well.

The Nyquist plots of copper in 0.5 mol l⁻¹ HCl containing 10⁻⁵ mol l⁻¹ cysteine at various immersion times are shown in Figure 6.

Comparing the two Nyquist diagrams, it is observed that the size of the semicircle after 24 h immersion is smaller than that after 4 h immersion. This suggests that the corrosion protection of cysteine for copper changed with time of immersion and reached a slightly decreased value after 24 h.

From the present investigation, it can be seen that cysteine has better protection effects for copper corrosion in a 0.5 mol l⁻¹ HCl solution compared with alanine and BTA. It is evident that the mercapto group in the cysteine molecular structure plays a key role. It is well known that the S atom has a strong adsorption affinity for copper [25]. The adsorption of the mercapto group on the copper surface is attributed to the 3d orbital of the S atom. The 3d orbital of the S atom extends far from the nuclei, and the electrons in the 3d orbital can easily be offered because the force by which they are attracted to the nuclei is small [26]. It is reported that the easier the offer of electrons from the inhibitor to the unoccupied d orbital of copper, the greater the inhibition efficiency [27]. Thus, the better inhibition efficiency of cysteine for copper corrosion in HCl can be attributed to the mercapto group in its molecular structure.

Table 2. Charge transfer resistance (R_t) and double layer capacitance (C_{dl}) of a copper electrode in 0.5 mol l⁻¹ HCl after 4 h immersion

Inhibitor	$R_t/k\Omega \text{ cm}^2$	$C_{dl}/\mu \text{ cm}^{-2}$
Blank	1.22	115.8
10 ⁻⁵ mol l ⁻¹ BTA	2.11	53.0
10 ⁻⁵ mol l ⁻¹ Alanine	3.10	40.1
10 ⁻⁵ mol l ⁻¹ Cysteine	3.40	35.2

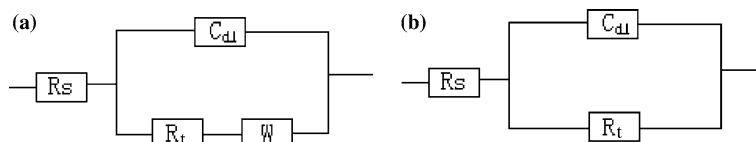


Fig. 5. Equivalent circuit model for the corrosion of copper: (a) displaying a Warburg impedance; (b) displaying a capacitive loop.

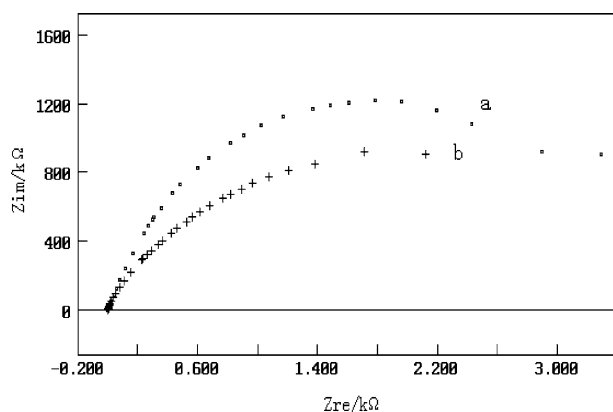


Fig. 6. Variation of Nyquist plots of a copper electrode in 0.5 mol l^{-1} HCl with $10^{-5} \text{ mol l}^{-1}$ cysteine after different immersion times: 4 h (a) and 24 h (b).

4. Conclusion

BTA, alanine, and cysteine have inhibitory effects on the anodic dissolution of copper in 0.5 mol l^{-1} HCl solution. Inhibition efficiencies of alanine and cysteine were higher than that of BTA, and cysteine was much more effective than alanine in acidic chloride solution. The presence of cysteine renders E_{cor} more positive and strongly decreases the anodic current density for copper corrosion. The improved inhibition efficiency of cysteine in 0.5 mol l^{-1} HCl solution can be attributed to adsorption on the copper surface by a mercapto group in its molecular structure, which forms a blocking barrier to copper corrosion.

Acknowledgement

The authors express their appreciation for support from the Shanghai Leading Discipline Project (P1304), P. R. China.

References

1. F. Mansfeld, T. Smith and E.P. Parry, *Corrosion* **27** (1971) 289.
2. F. Zucchi, G. Trabanelli and C. Monticelli, *Corros. Sci.* **38** (1996) 147.
3. T. Notoya and W. Poling, *Corrosion* **32** (1976) 216.
4. D. Chadwick and T. Hashemi, *Corros. Sci.* **18** (1978) 39.
5. F. El-Taib and S. Haruyama, *Corros. Sci.* **20** (1980) 887.
6. Y.C. Wu, P. Zhang, H.W. Pickering and D.L. Allara, *J. Electrochem. Soc.* **140** (1993) 2791.
7. V. Otieno-Alego, G.A. Hope, T. Notoya and D.P. Schweinsberg, *Corros. Sci.* **38** (1996) 213.
8. D.P. Schweinsberg, S.E. Bottle and V. Otieno-Alego, *J. Appl. Electrochem.* **27** (1997) 161.
9. N. Huynh, S.E. Bottle, T. Notoya and D.P. Schweinsberg, *Corros. Sci.* **42** (2000) 259.
10. M. Ohsawa and W. Suetaka, *Corros. Sci.* **19** (1979) 709.
11. D.Q. Zhang, L.X. Gao and G.D. Zhou, *J. Appl. Electrochem.* **33** (2003) 361.
12. D-Q. Zhang, L-X. Gao and G-D. Zhou, *Appl. Surf. Sci.* **225** (2004) 287.
13. E. Stupnisek-Lisac, A. Loncaric Bozic and I. Cafuk, *Corrosion* **54** (1998) 713.
14. R. Gasparac and E. Stupnisek-Lisac, *Corrosion* **55** (1999) 1031.
15. G. Moretti, F. Guidi and G. Grion, *Corros. Sci.* **46** (2004) 387.
16. D. Tromans and J.C. Silva, *J. Electrochem. Soc.* **143** (1996) 458.
17. D. Tromans and J.C. Silva, *Corrosion* **53** (1997) 171.
18. T. Aben and D. Tromans, *Electrochem. Soc.* **142** (1995) 398.
19. D. Tromans and T. Ahmed, *Electrochem. Soc.* **145** (1998) 601.
20. C.Y. Yan, H.C. Lin and C.N. Cao, *Electrochimica Acta* **45** (2000) 2845.
21. H. Ma, S. Chen, L. Niu, S. Zhao, S. Li and D. Li, *J. Appl. Electrochem.* **32** (2002) 65.
22. S.L. Li, H.Y. Ma, S.B. Lei, R. Yu, S.H. Chen and D.X. Liu, *Corrosion* **54** (1998) 947.
23. G.P. Cicileo, B.M. Rosales, F.E. Varela and J.R. Vilche, *Corros. Sci.* **40** (1998) 1915.
24. K. Hladky, L.M. Callow and J.L. Dawson, *Br. Corros. J.* **15** (1980) 20.
25. R. Tremont, H. De Jesus-Cardona, J. Garcia-Orozco, R.J. Castro and C.R. Cabrera, *J. Appl. Electrochem.* **30** (2000) 737.
26. D.Q. Zhang, L. Yu and Z. Lu, *J. Chin. Soc. Corros. Prot.* **18** (1998) 307.
27. D. Wang, S. Li, Y. Ying and M. Wang, *Corros. Sci.* **41** (1999) 1911.